Jurnal Engine:
Energi, Manufaktur, dan Material
Vol.9 No.2 November 2025 hal: 237 - 248

The Simulation of Radiation Shielding Made of Portland Material in a 230 MeV 300 NA Cyclotron Room for Proton Therapy Facility Using PHITS Code System

***Damar Adhiwidya Suyanto*[1]**
***Aditya Tri Oktaviana*[2]**
***Yohannes Sardjono*[3]**
***Gede Sutresna Wijaya*[4]**
***Isman Mulyadi Triatmoko*[5]**

[1,2,3,4,5]*Physics Study Program, Indonesia Defense University, Kawasan IPSC Sentul, Bogor Regency, West Java*
[1]*Author correspondence: damar.suyanto@mipa.idu.ac.id*

Article Info: *Received: July 07, 2025; Accepted: November 10, 2025; Available online: November 21, 2025*
DOI: *10.30588/jeemm.v9i2.2339*

Abstract: *This study investigates the effectiveness of radiation shielding made from Portland material in a 230 MeV, 300 NA cyclotron room for a proton therapy facility. Proton therapy is an advanced treatment method for cancer that uses protons to irradiate tumors with high precision. However, the high energy of protons requires effective shielding to protect the surrounding environment and personnel from radiation exposure. In this research, the radiation shielding performance of Portland material was evaluated using the PHITS (Particle and Heavy Ion Transport System) version 3.351 simulation software. The study focuses on assessing the attenuation of radiation within the cyclotron room under various operational conditions. The results from PHITS simulations provide insights into the potential of Portland material in reducing radiation levels in proton therapy rooms, contributing to the safety and efficiency of such facilities. This analysis is essential for optimizing shielding design.*

Keywords: *Portland Material, Proton Therapy, PHTS, Radiation attenuation, Safety analysis*

Abstrak: Penelitian ini menyelidiki efektivitas pelindung radiasi yang terbuat dari material Portland di ruang siklotron 230 MeV, 300 NA untuk fasilitas terapi proton. Terapi proton merupakan metode pengobatan kanker canggih yang memanfaatkan proton untuk meradiasi tumor dengan tingkat presisi yang sangat tinggi. Proses ini memungkinkan penghancuran sel kanker yang lebih tepat, namun energi proton yang tinggi juga menimbulkan risiko paparan radiasi pada lingkungan sekitar dan tenaga medis. Oleh karena itu, diperlukan pelindung radiasi yang efektif untuk memastikan keselamatan di ruang terapi. Dalam penelitian ini, kinerja pelindung radiasi dari material Portland dievaluasi dengan menggunakan perangkat lunak simulasi PHITS (Particle and Heavy Ion Transport System) versi 3.351. Simulasi ini bertujuan untuk menilai sejauh mana material Portland dapat mengurangi tingkat radiasi di ruang siklotron dalam berbagai kondisi operasional, seperti perubahan energi dan intensitas radiasi. Hasil simulasi PHITS menunjukkan bahwa desain pelindung material Portland, dengan ketebalan bervariasi antara 100 cm hingga 350 cm , berhasil menekan laju dosis radiasi total hingga di bawah batas aman regulasi BAPETEN, yaitu 0,25 µSv/jam . Studi ini sangat penting untuk mengoptimalkan desain pelindung di fasilitas terapi proton.

Kata Kunci: Material Portland, Terapi Proton, PHITS, Pengurangan Radiasi, Analisis Keselamatan.

I. Introduction

The effectiveness of radiation shielding in proton therapy facilities, particularly using Portland cement as a primary construction material, is critical in minimizing radiation exposure for both patients and healthcare workers. Recent advancements in computational simulations, particularly through the use of the Particle and Heavy Ion Transport code System (PHITS), underscore the significance of shielding design and its modeling for proton therapies.

Proton therapy benefits from a unique advantage over conventional photon therapies due to the distinct Bragg peak phenomenon, which localizes dose delivery to tumors while sparing surrounding healthy tissues [1]. However, this advantage necessitates robust shielding practices to protect against secondary radiation, including neutrons and gammas produced during treatment [2]. Studies have shown that secondary neutron doses can lead to significant exposure for personnel if shielding is not adequately designed[3]. Monte Carlo simulation tools, such as PHITS, are instrumental in optimizing this aspect by enabling researchers to evaluate designs comprehensively, including radiation interactions with different materials.

Several studies have demonstrated the comparative effectiveness of proton versus photon therapy. Notably, Baumann et al. conducted a study highlighting the lower observed toxicity in patients undergoing proton therapy relative to those receiving photon therapy as part of concurrent chemoradiotherapy for locally advanced cancer, suggesting that the higher upfront cost of proton therapy may be offset by cost savings from reduced hospitalizations and enhanced productivity from patients and caregivers [4]. Furthermore, a systematic review by Chen et al. underscored the benefits of modern delivery techniques such as intensity-modulated proton therapy (IMPT), which effectively mitigates the exposure of normal tissues while achieving accurate tumor targeting, which is pivotal for higher clinical outcomes [5].

Cost-effectiveness analyses have also positioned proton therapy favorably within the landscape of cancer treatments. Brodin et al. discussed the potential for proton therapy to offer individualized quality of life benefits and reduced rates of emergency room visits, indicating that these reductions in unplanned hospitalizations may contribute significantly to the overall cost-effectiveness of proton therapy for patients with oropharyngeal cancer [6]. In a broader context. evaluated the economic implications of proton therapy for head and neck cancers, reinforcing that while the upfront costs are significant, the long-term value gained through minimized treatment-related complications can provide substantial overall cost savings [7].

Moreover, recent investigations into biologically enhanced therapies are gaining traction, suggesting an adjunctive approach using boron compounds. For instance, Tabbakh et al. highlighted the potential for boron nanoparticles to enhance proton therapy's efficacy, indicating that the nuclear interactions facilitated by these compounds could significantly increase therapeutic outcomes [8]. Similarly, Popov et al. explored the molecular mechanisms by which boron compounds could sensitize tumor cells to proton therapy, presenting a promising avenue for further research [9].

The exploration of advanced simulation tools and techniques further highlights the evolving landscape of proton therapy. Gao et al. emphasized the necessity of accurate proton range estimation to mitigate uncertainties in dose delivery, proposing the use of deep learning frameworks for generating synthetic dose-weighted linear energy transfer (LET) maps that could enhance treatment planning accuracy [10]. Such advancements are crucial as they improve the precision of targeting, a hallmark of proton therapy's clinical effectiveness.

In conclusion, the literature underscores a robust optimism surrounding proton therapy characterized by its clinical efficacy, potential for reduced toxicity, and advancements in complementary technologies. The continued research and development in this field not only bolster therapeutic outcomes but also provide a pathway towards enhanced quality of life for patients undergoing cancer treatment.

II. Material and Methods

The instrumentation used to run a series of simulations in this research includes a portable computer, specifically a Macbook Pro M1 Pro equipped with the M1 Pro chipset, 16GB of RAM, and running on the Mac Sequoia 15.4 Operating System. The simulations were conducted using the PHITS simulation program, version 3.51, which is essential for modeling particle transport and radiation shielding. Additional tools utilized in this research include Microsoft Word 2021 and Microsoft Excel 2021 for documentation and data analysis. The PHITSPAD_launch and EPSPDF programs were used for launching and processing simulations, while Ghostscript was employed for handling PDF file conversions.

1. Cyclotron 230 MeV Design

In this study, the S2C2 cyclotron with an energy of 230 MeV is used as the primary particle source for proton therapy simulations in a shielding room. The S2C2 cyclotron, designed to accelerate protons to an energy of 230 MeV, plays a pivotal role in delivering high-energy protons to the treatment area. For the purpose of this research, the cyclotron is modeled within the simulation environment to assess its interaction with the shielding materials. The shielding room is specifically designed to protect personnel and surrounding areas from radiation exposure, and it is equipped with various protective materials to attenuate the proton beam as it moves from the cyclotron to the treatment room. The simulation takes into account the cyclotron's geometry, the proton beam extraction system, and the energy spectrum of the protons, enabling a detailed evaluation of the radiation shielding effectiveness in a proton therapy facility

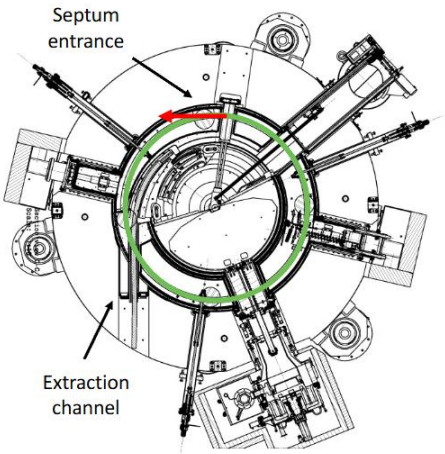

Figure 1. The illustration shows two sources of proton losses in the S2C2, simulated in BDSIM: uniformly distributed losses along the accelerator's circumference (green) and losses at the septum (red) [11].

2. Design of Shielding Room for Proton Therapy

The design of the shielding room for proton therapy consists of several key areas, each serving a specific purpose in the overall treatment process. The cyclotron room is the first component, housing the S2C2 cyclotron, where protons are accelerated to high energies before being directed towards the treatment rooms. The first treatment room, Treatment Room 1, is where the proton therapy takes place, with the proton beam delivered precisely to the tumor site for therapeutic purposes. Treatment Room 2 is designated as the patient and radiologist entry area, providing a space for patient preparation and positioning before entering Treatment Room 1. Effective shielding is incorporated into all these spaces to minimize radiation exposure to personnel and surrounding areas while ensuring the safety and efficacy of the proton therapy process.

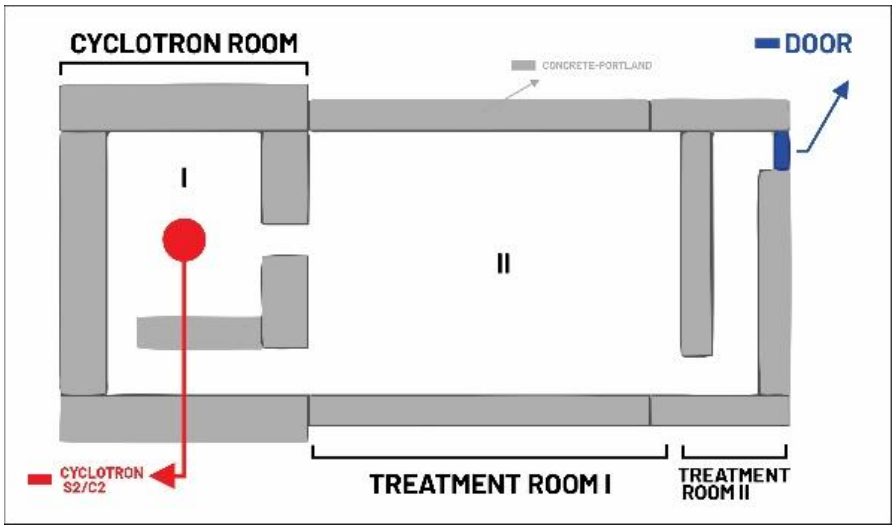

Figure 2. Design of shielding room with PHITS

3. Spatial Geometry of Accelerators

The facility is divided into three distinct rooms with specific functions. The first room, measuring 9 m × 5 m × 3 m, is where the cyclotron accelerator is located. Adjacent to it is the second room, which spans 20 m × 5 m × 3 m and serves as the beam transport system area. The third room, measuring 9 m × 2 m × 3 m, acts as the entrance to the second room and provides access to the beam transport system. All three rooms are surrounded by shielding materials to ensure safety, and the entrance is equipped with a plug door made of barite concrete, which is coated with carbon steel. This design provides essential protection against radiation for both the system and its users.

The calculation of radiation doses for each wall is divided according to the numbered sections indicated in Figures 3 and 4. These figures provide a detailed breakdown of the dose distribution, allowing for a clear understanding of the shielding requirements for each specific wall in the facility [12]. The numbers correspond to different areas, helping to identify the precise radiation protection measures necessary for each section[13].

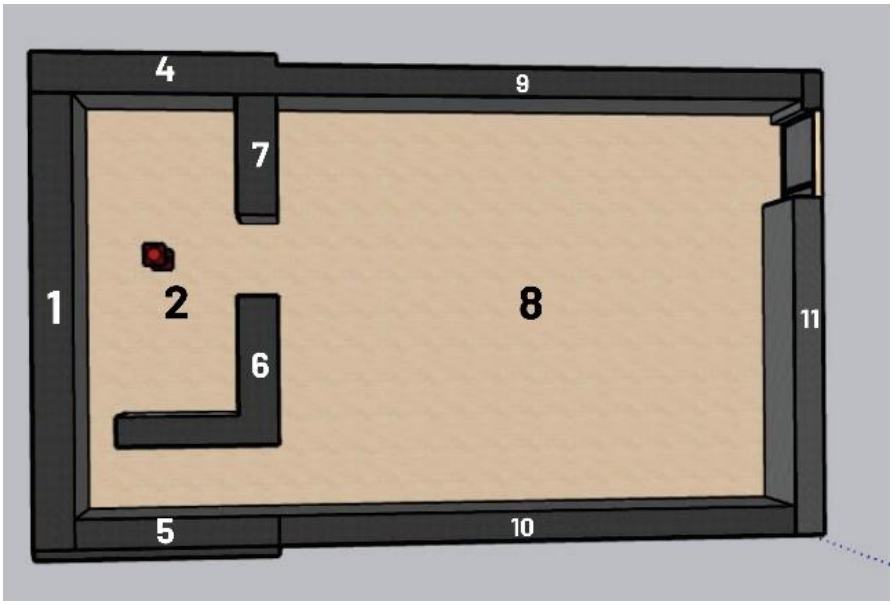

Figure 3. Room Geometry in axial view

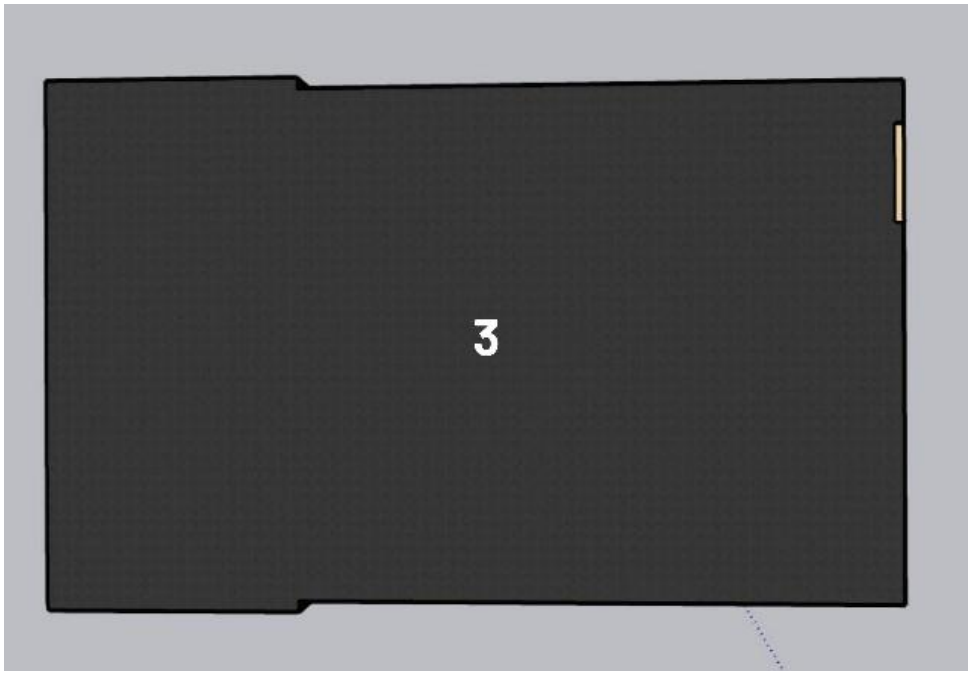

Figure 4. The roof of the shielding room.

The spatial division of the facility is outlined, focusing on the wall configuration of three primary rooms: the cyclotron room, the beam transport system room, and the treatment room. Each room plays a crucial role in the overall operation of the accelerator system. The walls are numbered to indicate their specific location and function within the facility, with careful attention given to shielding and accessibility. Below is the breakdown of each wall based on its position in the respective rooms.

1) **Wall 1**: The back of the cyclotron, serving as the rear boundary of the cyclotron room.
2) **Wall 2**: The floor of the cyclotron room, providing the foundation for the equipment within this area.
3) **Wall 3**: The roof of the entire shielding room, offering protection against radiation from above.
4) **Wall 4**: The right side of the cyclotron in the cyclotron room, marking the right boundary of the space housing the cyclotron.
5) **Wall 5**: The left side of the cyclotron in the cyclotron room, marking the left boundary of the cyclotron area.
6) **Wall 6**: The left side of the beam transport system, acting as the left boundary for the beam's pathway.
7) **Wall 7**: The right side of the beam transport system, serving as the right boundary of the beam's transport area.
8) **Wall 8**: The floor of the beam transport system room, forming the base on which the beam transport system operates.
9) **Wall 9**: The right side of the treatment room, marking the right boundary of the therapy space.
10) **Wall 10**: The left side of the treatment room, defining the left boundary of the therapy room.
11) **Wall 11**: The front of the entrance to the treatment room, allowing access to the therapy area from the main passageway.

4. Research Variables

This study, the research variables are the type of material and the material thickness. The type of material used is Portland cement. The composition of various shielding materials based on atomic fraction, as referenced from the *Compendium of Material Composition Data for Radiation Transport Modelling*, is shown in the table [14]. These materials play a crucial role in ensuring the effectiveness of radiation shielding and contribute to accurate radiation transport modeling.

Table 1. Composition of radiation shielding materials [14]

Material Component	Portland Cement (ρ = 2,35 g/cm³)
H	16.875
C	0.142
O	56.253
Na	1.184
Mg	0.14
Al	2.135
Si	20.412
S	
K	0.566
Ca	1.867
Fe	0.426
Ba	

5. Analysis of Research Results

The PHITS simulation results provide the dose rate. The dose rate value is obtained by converting the particle flux using the multiplier 202 command, which aligns with the ICRP 103 from 2007. The output from the multiplier is measured in pSv, which is then converted to μSv by multiplying it by 10^{-6} [15].

The variables in this study are the type and thickness of the material. For each material, the thickness is varied to determine the dose rate that meets the regulations set by BAPETEN Regulation No. 3 of 2013. In this study, it is assumed that the general public is exposed for 2000 hours per year. The maximum dose for the general public is determined by the following equation (1.1).

$$Exposure\ time = 8\frac{hour}{day} \times 5\frac{day}{week} \times 50\frac{week}{year} = 2000\frac{hour}{year} \quad (1)$$

$$Maximum\ dose = \frac{500\mu Sv/year}{2000\ hour/year} = 0.25\mu Sv/hour \quad (1.1)$$

III. Result and Discussion

The thickness and dose rate for each wall in the Portland cement shield design are listed in the following table.

Table 2. The dose rate on the Portland concrete shield wall

Wall Thickness (cm)	Total Dose Rate (μSv/hour)	Proton Dose Rate (μSv/hour)	Neutron Dose Rate (μSv/hour)	Photon Dose Rate (μSv/hour)
1 (190)	2.060 x 10^-1	0	1.909 × 10^-1	1.169 × 10^-2
2 (200)	1.829 x 10^-1	8.900 × 10^-3	1.525 × 10^-1	4.031 × 10^-3
3 (150)	1.544 x 10^-1	0	1.496 × 10^-1	4.731 × 10^-3
4 (220)	8.656 x 10^-2	0	5.626 × 10^-2	1.459 × 10^-3
5 (170)	5.793 x 10^-2	2.002 × 10^-5	5.626 × 10^-2	7.425 × 10^-3
6 (350)	2.193 x 10^-3	8.924 × 10^-5	2.182 × 10^-3	9.560 × 10^-4
7 (350)	2.065 x 10^-1	7.684 × 10^-5	1.354 × 10^-1	1.022 × 10^-3

8 (200)	2.216 x 10^-1	6.900 × 10^-3	2.088 × 10^-3	3.688 × 10^-3
9 (150)	9.213 x 10^-3	0	9.141 × 10^-3	7.048 × 10^-3
10 (150)	2.356 x 10^-2	0	5.022 × 10^-2	5.022 × 10^-2
11 (100)	2.343 x 10^-2	2.223 × 10^-3	2.223 × 10^-3	1.194 × 10^-3

As shown in Table 2, there are significant variations in dose rates that do not correlate linearly solely with wall thickness. For instance, Wall 7 (350 cm thick) exhibits a total dose rate (2.065 x 10^{-1} µSv/h) that is significantly higher than that of Wall 9 (150 cm thick) (9.213 x 10^{-3} µSv/h). Similarly, walls of identical thickness, such as Walls 9 and 10 (both 150 cm), display significantly different dose rates.

These observed fluctuations can be attributed to the specific location and function of each wall relative to the radiation source (cyclotron) and the proton beam path. Walls located closer to the source or serving as primary shielding (such as Walls 6 and 7) are exposed to a significantly higher particle flux, thereby necessitating greater thickness for attenuation. Conversely, walls situated further from the source (such as Wall 9) can achieve safe dose rates with reduced thickness.

A more detailed analysis of the following figures will outline the dose rates for each specific location. The key finding is that the selected thicknesses for each location (ranging from 100 cm to 350 cm) proved successful in reducing the total dose rate to below the safe threshold of 0.25 µSv/h established by BAPETEN.

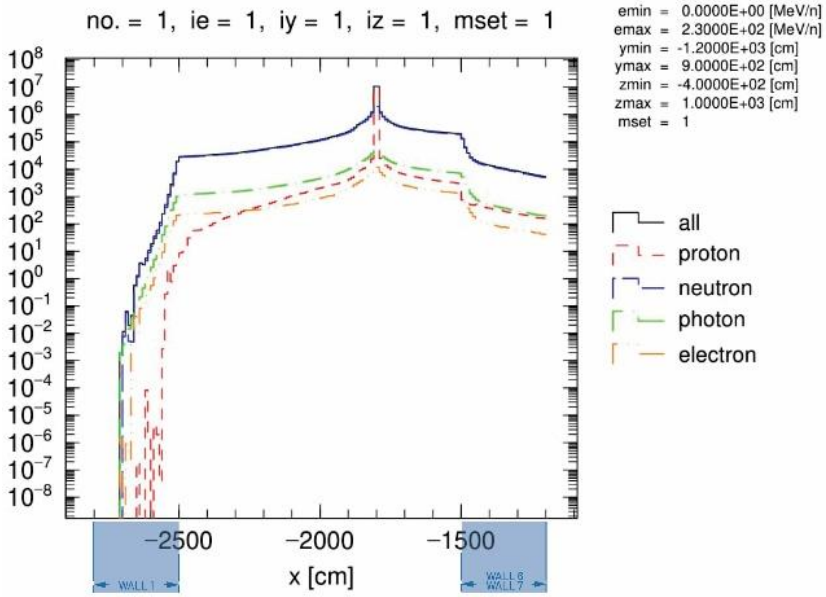

Figure 5. Graph of dose rate on the X-axis of cyclotron room

Figure 5 illustrates the dose rate on walls 1, 6, and 7, aligned with the Z-axis. The proton source is located on the Z-axis, where the protons begin to interact with the air until they reach the shield walls at Z = -2800 and Z = -2500. The protons then interact with the shield walls, and after a certain thickness, they produce dose rate values that comply with regulations. Wall 1, with a thickness of 185 cm, can attenuate radiation to a value of 0.206 µSv/hour. Walls 6 and 7, with a thickness of 350 cm, can attenuate radiation to values of 0.2193 and 2.065 µSv/hour, respectively. Walls 6 and 7 are primary shield walls with high particle flux, requiring a large thickness to effectively attenuate radiation.

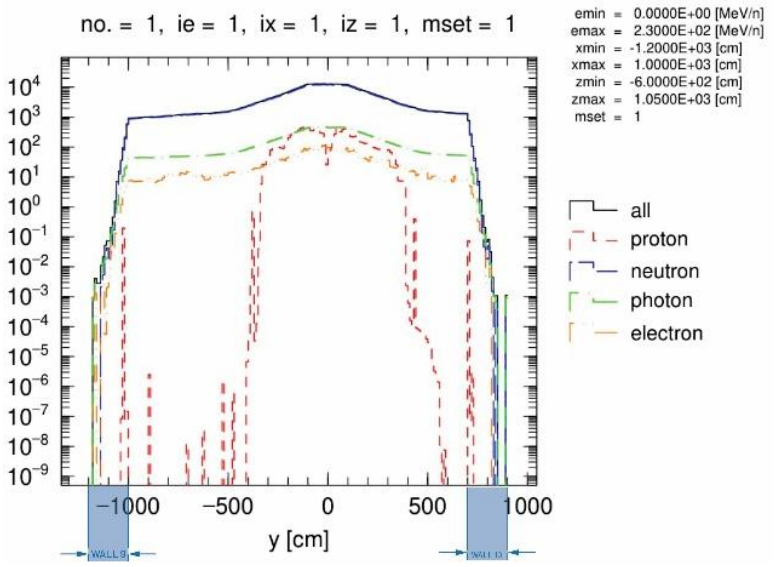

Figure 6. Graph of dose rate on the Y-axis of treatment room 2

Figure 6 depicts the dose rate on wall 11, which spans the Z-axis range from Z = 1700 to Z = 1900. This wall, with a thickness of 100 cm, is designed to attenuate radiation to a dose rate of 0.0343 µSv/hour. Wall 11 serves as the shielding for the proton therapy treatment room entrance. Given its strategic location, this wall plays a crucial role in minimizing radiation exposure for individuals entering the treatment room. The chosen thickness effectively reduces the radiation levels to meet safety standards, ensuring that the entrance remains safe for both patients and staff.

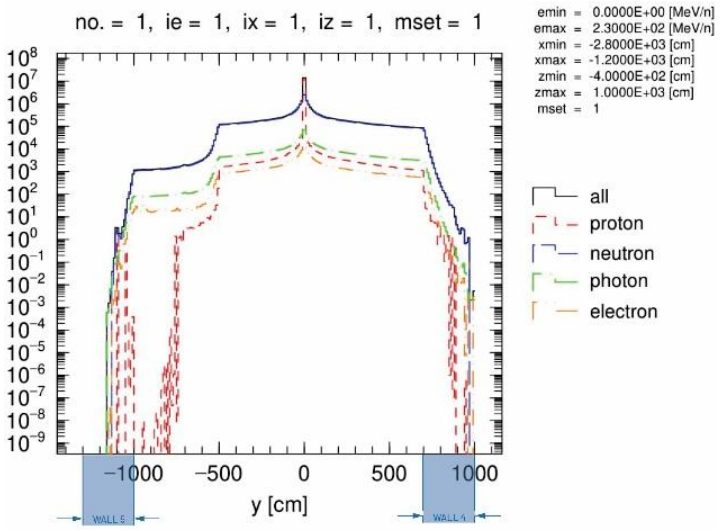

Figure 7. Graph of dose rate on the Y-axis of cyclotron room

Figure 7 shows the dose rate on walls 4 and 5, with wall 4 covering the Z-axis range from Y = 700 to Y = 1000 and wall 5 spanning Y = 1000 to Y = 1300. Wall 4, with a thickness of 220 cm, effectively attenuates radiation to a dose rate of 0.0856 µSv/hour. On the other hand, wall 5, with a thickness of 170 cm, reduces radiation to a dose rate of 0.0579 µSv/hour. Wall 4 needs to be thicker because it is located closer to the right side of the cyclotron, where radiation levels are higher due to the proximity to the proton source. Wall 5, being farther to the left of the cyclotron, does not require as much shielding thickness, as the radiation intensity decreases with distance from the source. The varying thicknesses of

these walls ensure that radiation exposure is minimized in both areas, meeting safety standards for the facility.

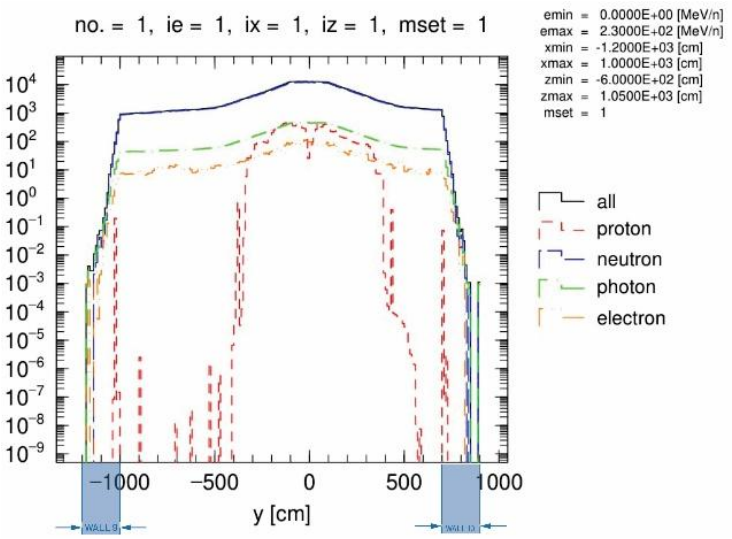

Figure 8. Graph of dose rate on the Y-axis of Treatment room 1

Figure 8 illustrates the dose rate on walls 9 and 10, with wall 9 covering the Y-axis range from Y = -1200 to Y = -1000. Wall 9, with a thickness of 150 cm, effectively attenuates radiation to a dose rate of 0.009213 µSv/hour. This wall is located in Treatment Room 1, where proton therapy is conducted. Similarly, wall 10, also with a thickness of 150 cm, attenuates radiation to a higher dose rate of 0.02356 µSv/hour.

Wall 10 experiences a higher dose rate attenuation because it is positioned closer to the direction of the proton beam during therapy, where radiation exposure is more intense. Both walls play crucial roles in shielding the treatment rooms, ensuring the safety of patients and staff by reducing radiation exposure to acceptable levels according to safety standards. The varying attenuation levels are accounted for by the different proximities to the proton beam, with wall 10 requiring more shielding due to its closer location to the beam's path.

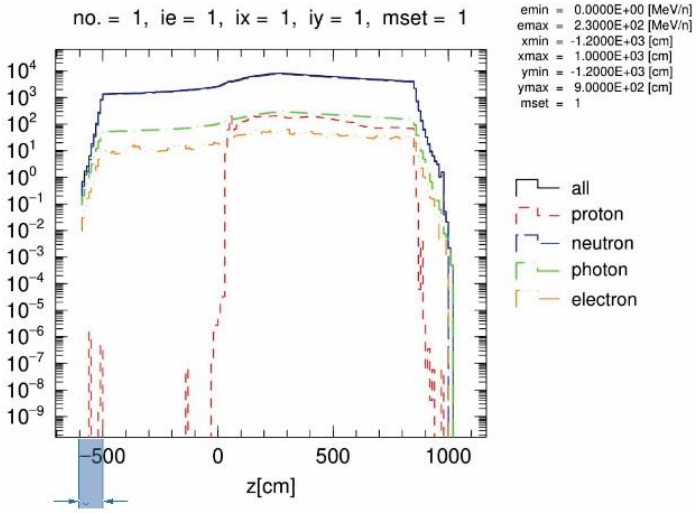

Figure 9. Graph of dose rate on the Z-axis of roof cyclotron room

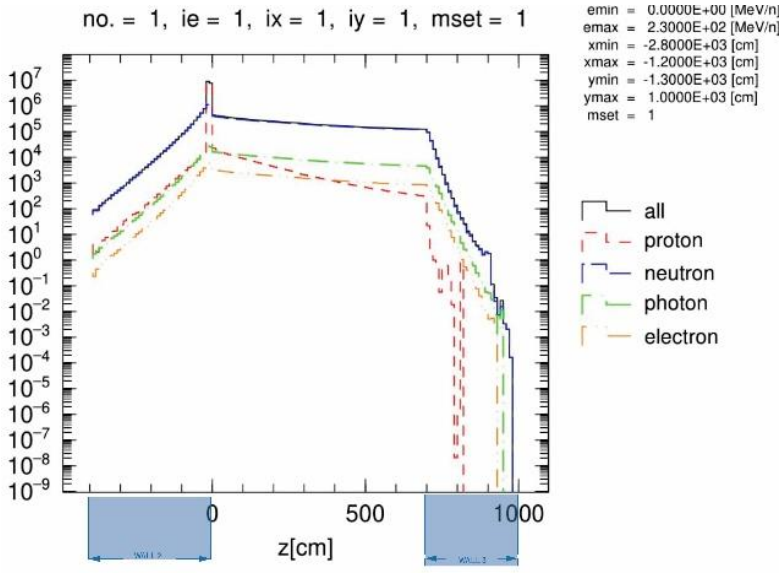

Figure 10. Graph of dose rate on the Z-axis of floor cyclotron room

Figure 9 presents the dose rate on the ceiling of the cyclotron room, where the shielding has a thickness of 150 cm, effectively attenuating radiation to a dose rate of 0.1544 µSv/hour. Since this is the ceiling, it does not pose a direct risk to people or staff, as there is no one typically present in this area. The ceiling's purpose is mainly to limit radiation exposure to any potential overhead equipment or external areas, ensuring the safety of the facility as a whole.

Figure 10 shows the dose rate on the floor of the cyclotron room for wall 2, and the floor of Treatment Room 1 for wall 8, both with a shielding thickness of 200 cm. Wall 2, located in the cyclotron room, can attenuate radiation to a dose rate of 0.1829 µSv/hour. Wall 8, in Treatment Room 1, reduces the dose rate to 0.2216 µSv/hour.

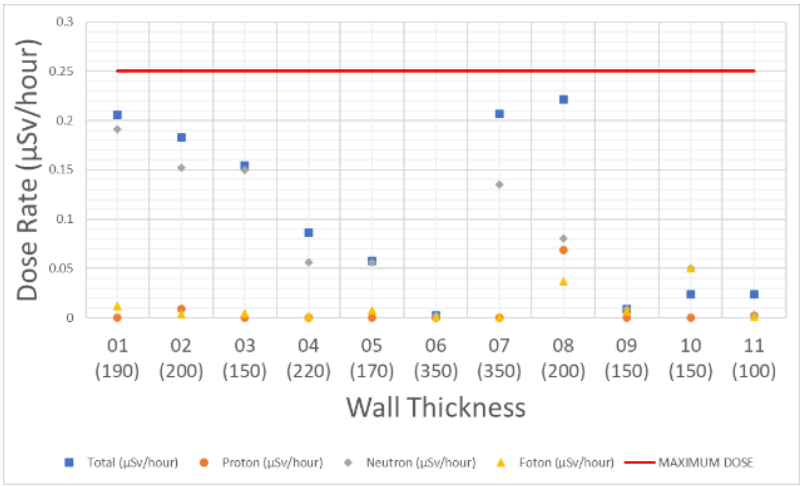

Figure 11. The dose rate graph of the Portland cement shielding design.

Portland cement is the most commonly used shielding material for radiation protection. This material is easily available in Indonesia due to its standardization in SNI. With a density of 2.35 g/cm³, Portland cement has the lowest density compared to other materials. Additionally, it contains relatively few high atomic number atoms. The concept of radiation attenuation is that a high atomic number and

density result in thicker Portland cement shield walls compared to other shielding designs. A comparison of the dose rate values on each wall against the dose limit based on BAPETEN regulations is shown in Figure 11.

Neutron radiation contributes the most to the total dose rate. This aligns with the research conducted. The thickness of each wall results in dose rate values that fall within the safe limits set by BAPETEN, which is 0.25 μSv/hour. The thickness of each wall ensures that the dose rate remains within the safe limit established by BAPETEN, confirming the adequacy of the shielding design.

IV. Conclusion

Based on the measurements of wall thickness and the radiation dose rate provided in the table and graph, it can be concluded that the radiation protection in the proton therapy room with 230 MeV energy is within safe limits. The total radiation dose detected at all tested wall thicknesses, which range from Wall 1 (190 cm) to Wall 11 (100 cm), remains below the threshold value recommended by BAPETEN, which is 0.25 μSv/hour. No dose rate exceeds this value for any of the wall thicknesses, indicating that the radiation protection applied in the proton therapy room is effective in reducing radiation exposure. Therefore, it can be concluded that the proton therapy room meets the radiation safety standards and poses no significant risk to personnel in the surrounding area.

Acknowledgment

We would like to extend our sincere thanks and appreciation to the Department of Physics, Faculty of Mathematics and Natural Sciences, University of Jember, and the Research Centre for Nuclear Safety, Metrology, and Quality Technology, National Research and Innovation Agency, for their invaluable support throughout the course of this research.

Reference

[1] T. Depuydt, “Proton therapy technology evolution in the clinic: impact on radiation protection.”

[2] S. Matsumoto, Y. Koba, R. Kohno, C. Lee, W. E. Bolch, and M. Kai, “Secondary neutron doses to pediatric patients during intracranial proton therapy: Monte Carlo simulation of the neutron energy spectrum and its organ doses,” *Health Phys*, vol. 110, no. 4, pp. 380–386, 2016, doi: 10.1097/HP.0000000000000461.

[3] R. Adinda and H. Gultom, “STUDY OF VARIATIONS IN RADIATION SHIELDING MATERIALS IN A 230 MEV 300 NA CYCLOTRON ROOM FOR PROTON THERAPY FACILITIY USING PHITS.” [Online]. Available: http://etd.repository.ugm.ac.id/

[4] B. C. Baumann *et al.*, “Comparative Effectiveness of Proton vs Photon Therapy as Part of Concurrent Chemoradiotherapy for Locally Advanced Cancer,” *JAMA Oncol*, vol. 6, no. 2, pp. 237–246, Feb. 2020, doi: 10.1001/jamaoncol.2019.4889.

[5] Z. Chen, M. M. Dominello, M. C. Joiner, and J. W. Burmeister, “Proton versus photon radiation therapy: A clinical review,” 2023, *Frontiers Media S.A.* doi: 10.3389/fonc.2023.1133909.

[6] N. P. Brodin *et al.*, “Individualized quality of life benefit and cost-effectiveness estimates of proton therapy for patients with oropharyngeal cancer,” *Radiation Oncology*, vol. 16, no. 1, Dec. 2021, doi: 10.1186/s13014-021-01745-1.

[7] D. Huang *et al.*, "Cost-effectiveness models of proton therapy for head and neck: Evaluating quality and methods to date," *Int J Part Ther*, vol. 8, no. 1, pp. 339–353, Jun. 2021, doi: 10.14338/IJPT-20-00058.1.

[8] F. Tabbakh, N. S. Hosmane, S. M. Tajudin, A. H. Ghorashi, and N. Morshedian, "Using 157Gd doped carbon and 157GdF4 nanoparticles in proton-targeted therapy for effectiveness enhancement and thermal neutron reduction: a simulation study," *Sci Rep*, vol. 12, no. 1, Dec. 2022, doi: 10.1038/s41598-022-22429-0.

[9] A. L. Popov *et al.*, "Boron Nanoparticle-Enhanced Proton Therapy: Molecular Mechanisms of Tumor Cell Sensitization," *Molecules*, vol. 29, no. 16, Aug. 2024, doi: 10.3390/molecules29163936.

[10] M. Goitein, "Calculation of the uncertainty in the dose delivered during radiation therapy," *Med Phys*, vol. 12, no. 5, pp. 608–612, 1985, doi: 10.1118/1.595762.

[11] E. Ramoisiaux *et al.*, "Concrete shielding activation for proton therapy systems using BDSIM and FISPACT-II," in *Journal of Physics: Conference Series*, Institute of Physics, 2023. doi: 10.1088/1742-6596/2420/1/012064.

[12] Y. Shang *et al.*, "Multilayer polyethylene/ hexagonal boron nitride composites showing high neutron shielding efficiency and thermal conductivity," *Composites Communications*, vol. 19, pp. 147–153, Jun. 2020, doi: 10.1016/j.coco.2020.03.007.

[13] S. N. Penfold, "Radiation shielding assessment of high-energy proton imaging at a proton therapy facility," *Med Phys*, vol. 49, no. 8, pp. 5340–5346, Aug. 2022, doi: 10.1002/mp.15727.

[14] "Data Mining Analysis and Modeling Cell Compendium of Material Composition Data for Radiation Transport Modeling," 2021. [Online]. Available: https://www.ntis.gov/about

[15] Icrp, "Annals of the ICRP Published on behalf of the International Commission on Radiological Protection."